

1 **Molecular phylogeny and historical biogeography of Apicotermitinae (Blattodea:**
2 **Termitidae)**

3 Johanna Romero Arias¹, Arthur Boom¹, Menglin Wang², Crystal Clitheroe², Jan Šobotník³, Petr Stiblík⁴,
4 Thomas Bourguignon^{2,3}, Yves Roisin¹

5
6 ¹ Evolutionary Biology & Ecology, Université libre de Bruxelles, Brussels, Belgium

7 ² Okinawa Institute of Science & Technology Graduate University, Okinawa, Japan

8 ³ Faculty of Tropical AgriSciences, Czech University of Life Sciences, Prague, Czech Republic

9 ⁴ Faculty of Forestry and Wood Sciences, Czech University of Life Sciences, Prague, Czech Republic

10

11 **Correspondence**

12 Johanna Romero Arias, Evolutionary Biology & Ecology,

13 Université libre de Bruxelles, 50 Avenue Franklin Roosevelt, Brussels 1050, Belgium.

14 Email: joharomeroa@gmail.com

15 Thomas Bourguignon, Okinawa Institute of Science & Technology Graduate University,

16 1919-1 Tancha, Onna-son, Okinawa

17 904-0495, Japan

18 Email : thomas.bourguignon@oist.jp

19

20 **Funding Information**

21 Belgian National Fund for Scientific Research F.R.S.-FNRS (PDR T.0065.15),

22 Van Buuren and Jaumotte–Demoulin fund,

23 subsidiary funding to Okinawa Institute of Science & Technology Graduate University,

24 Internal Grant Agency of the Faculty of Tropical Agrisciences CULS (20205014).

25

26 **Abstract**

27 Soil-feeding termites are abundant in tropical regions and play an important role in soil bioturbation and
28 in the organic matter cycle. The Apicotermitinae are arguably the most diverse lineage of soil-feeding
29 termites, but they are also the most understudied, probably because many species are soldierless, which
30 makes identification difficult. Although the backbone of the termite phylogenetic tree is now well-
31 resolved, the relationships among representatives of Apicotermitinae are still largely unknown. Here, we
32 present phylogenetic trees inferred from 113 mitochondrial genomes of Apicotermitinae representative of
33 the group diversity. Our analyses confirm the monophyly of the Apicotermitinae and the basal position of
34 soldiered taxa, within which two lineages of soldierless species are nested. We describe two new
35 monotypic genera, whose phylogenetic position appeared of special interest: *Koutabatermes* **gen. n.**, lies
36 on a long branch among soldiered taxa, and *Apolemotermes* **gen. n.**, is sister to *Adaiphrotermes*. We

37 resolved, with high support, the position of Asian genera as sister group of a clade comprising the
38 monophyletic neotropical *Anoplotermes*-group and the small African clade including *Adaiphrotermes* and
39 *Apolemotermes* **gen. n.**. Our trees cast light on the intergeneric and interspecific relationships within
40 Apicotermitinae and reveal the polyphyly of several genera, including *Ruptitermes*, *Astalotermes* and
41 *Anoplotermes*. Biogeographic reconstructions revealed two dispersal events out of Africa, one to the
42 Oriental realm and one to the Neotropical realm. Overall, the timing of Apicotermitinae diversification
43 and dispersal, following the Eocene-Oligocene boundary, matches that found for other groups of
44 Neoisoptera. Nomenclatural acts are registered in ZooBank:
45 <http://zoobank.org/urn:lsid:zoobank.org:pub:CA1A21B6-573E-4855-8C88-372453C922F7>.

46

47

48 **KEYWORDS**

49 humivorous, Isoptera, mitochondrial genome, molecular clock, systematics

50 **Introduction**

51 The Apicotermitinae is a subfamily of soil-feeding termites that play important roles in soil bioturbation
52 and organic matter cycling in tropical rainforests and savannas (Jones & Eggleton, 2011; Bourguignon *et*
53 *al.*, 2016b). This subfamily was originally erected by Grassé & Noirot (1955) for the African soldiered
54 taxa related to *Apicotermes* Holmgren, which were previously placed in the Termitinae. At that time, the
55 soldierless termites were classified in the Amitermitinae and were divided into two genera: *Anoplotermes*
56 Müller, which included the African species and most Neotropical species, and *Speculitermes* Wasmann,
57 which included the then-believed soldierless Asian species and some Neotropical species (Snyder, 1949).
58 Soon afterwards, Roonwal and Sen-Sarma (in Roonwal, 1958) erected the Indotermitidae family for the
59 soldiered genus *Indotermes* Roonwal & Sen-Sarma from South Asia, but Ahmad (1963) outlined the
60 close relatedness between *Indotermes* and *Speculitermes* and moved both genera to the Amitermitinae.
61 Soldiers were later discovered in one *Speculitermes* species (Roonwal & Chhotani, 1966), but remain
62 unknown, and are possibly absent, in several Oriental species. In his revision of African soldierless
63 termites, Sands (1972) expanded the Apicotermitinae subfamily and distinguished two 'branches': (i) the
64 *Apicotermes*-branch, including *Apicotermes* and related African soldiered genera; and (ii) the
65 *Anoplotermes*-branch, including the soldierless taxa, the soldiered genus *Firmitermes* Sjöstedt, and the
66 Oriental genera *Speculitermes*, *Indotermes* and relatives. More recently, based on gut anatomy, Noirot
67 (2001) recognized three 'groups': (i) the *Apicotermes*-group, including the soldiered African taxa and the
68 soldierless genus *Skatitermes* Coaton; (ii) the *Speculitermes*-group, including all Asian Apicotermitinae;
69 and (iii) the *Anoplotermes*-group, including the African and Neotropical soldierless species plus the
70 soldiered genus *Firmitermes*.

71 Soldierless species are very abundant in Africa and the Neotropics, where they can locally make up more
72 than 30% of the termite species diversity (Eggleton *et al.*, 1995, 2002; Bourguignon *et al.*, 2011, 2016b;
73 Dahlsjö *et al.*, 2015, 2020; Nduwarugira *et al.*, 2017). This makes the Apicotermitinae one of the most
74 diverse subfamilies of Termitidae. It is also the most understudied, probably because many species, being
75 soldierless, can only be distinguished morphologically by tedious and difficult dissections of the worker
76 digestive tract (Grassé & Noirot, 1955; Sands, 1972, 1998; Noirot, 2001; Bourguignon *et al.*, 2016b). The
77 shape of the mesenteron-proctodeum junction forming a mixed segment and the morphologically variable
78 enteric valve armature are the conventional characters used for the Apicotermitinae taxonomy (Grassé &
79 Noirot, 1955; Sands, 1972, 1998; Noirot, 2001). The gizzard ornaments are also useful as taxonomic
80 characters, particularly in the African soldierless species (Noirot, 2001; Romero Arias *et al.*, 2020). While
81 some genera are characterized by conspicuous apomorphies, such as the hypertrophied sclerotized
82 cushion 1 of the enteric valve in *Ateuchotermes* Sands, others mostly accommodate species that lack
83 particular diagnostic features, such as *Astratotermes* Sands, whose enteric valve lacks distinctive
84 characters (Sands, 1972).

85 Despite recent progress on the taxonomy of Neotropical Apicotermittinae (e.g. Bourguignon *et al.*, 2010,
86 2016a; Acioli & Constantino, 2015; Constantini *et al.*, 2018), the systematics of this subfamily remains
87 largely unresolved. To date, 224 species and 52 genera of Apicotermittinae have been described, with
88 diversity hotspots located in Africa and South America (Bourguignon *et al.*, 2016b; Constantino, 2020;
89 Roisin, 2021). However, the actual diversity of the group is much larger, and many species, still awaiting
90 formal description, have been informally labelled as morphospecies in ecological surveys (e.g. Eggleton
91 *et al.*, 1995, 2002; Davies, 2002; Bourguignon *et al.*, 2011; Nduwarugira *et al.*, 2017).

92 The first comprehensive phylogenetic study of termites was based on a combination of morphological
93 characters and genetic markers, including two mitochondrial genes (COII and 12S) and one nuclear gene
94 (28S) (Inward *et al.*, 2007). This study supported the monophyly of Apicotermittinae, which were
95 retrieved as the sister group of a clade composed of all other Termitidae except the fungus-growers
96 (Macrotermittinae) and the two small subfamilies Sphaerotermitinae and Foraminitermitinae (Inward *et*
97 *al.*, 2007). This phylogenetic position was later confirmed by molecular phylogenies inferred from
98 complete mitochondrial genomes and transcriptomes (Bourguignon *et al.*, 2015, 2017; Bucek *et al.*,
99 2019). In addition, the phylogenetic tree of Inward *et al.* (2007) suggested that (1) the African soldiered
100 taxa are paraphyletic to a clade composed of the soldierless lineages and the Asian (soldiered)
101 Apicotermittinae; (2) the Oriental *Speculitermes*-group is monophyletic; (3) the Neotropical
102 *Anoplotermes*-group is monophyletic; and (4) the Oriental *Speculitermes*-group, the Neotropical
103 *Anoplotermes*-group and the African soldierless genus *Adaiaphrotermes* Sands form a monophyletic group
104 sister to all other African soldierless taxa. This tree topology implies two independent losses of soldiers in
105 Apicotermittinae and two independent dispersal events between continents, with unclear directionality.
106 Complete mitochondrial genome phylogenies confirmed that Asian and Neotropical taxa are closer to
107 each other than most African soldierless genera (Bourguignon *et al.*, 2017). However, because of their
108 insufficient sampling, poor characterization of some described genera (e.g. *Astalotermes* Sands,
109 *Anenteotermes* Sands), and uncertain identifications, the history of Apicotermittinae remains unclear. In
110 addition, most relationships among African and Neotropical soldierless taxa were unresolved by Inward
111 *et al.* (2007), and several genera (e.g. *Aderitotermes* Sands, *Astalotermes* or *Anoplotermes*) appeared as
112 polyphyletic in the phylogenetic trees of Bourguignon *et al.* (2017).

113 In this study, we used 113 mitochondrial genomes of Apicotermittinae species to reconstruct robust
114 phylogenetic trees including most morphologically defined genera. Using these trees, we tested previous
115 phylogenetic hypotheses regarding the relationships among major Apicotermittinae clades and provided a
116 timeframe for their evolution. We also investigated the historical biogeography of Apicotermittinae and
117 determined the number of independent losses of soldiers. Our analyses clarify the taxonomy of
118 Apicotermittinae and pave the path to future taxonomic revisions of non-monophyletic genera, such as
119 *Astalotermes* or *Anoplotermes*, and provide a framework to study the anatomical evolution of the
120 subfamily.

121 **Material and methods**

122 ***Sampling***

123 Termite sampling was conducted in Burundi (n = 7), Cameroon (n = 28), Ivory Coast (n = 18), Kenya (n
124 = 1), French Guiana (n = 12) and Argentina (n = 1) (Table S1). For each sample, we collected specimens
125 in RNA-later® or in 100% ethanol for genetic analyses, and in 80% ethanol for morphological analyses.
126 Samples collected in RNA-later® and 100% ethanol were temporarily stored at a temperature ranging
127 from -20°C to 4°C, and shipped to the Czech University of Life Sciences or to the Okinawa Institute of
128 Science and Technology, where they were stored at -80°C until DNA extraction. Samples collected in
129 80% ethanol are stored at the Université Libre de Bruxelles and the Czech University of Life Sciences. In
130 addition to the 67 samples collected in this study, we also obtained the full mitochondrial genome
131 sequences of 43 samples of Apicotermitinae from GenBank (Bourguignon *et al.*, 2015, 2017) and
132 reconstructed mitochondrial genomes from transcriptome sequences of three species (Bucek *et al.*, 2019)
133 (Table S1).

134 Species identifications were based on morphological and anatomical characters, which included the
135 worker digestive tube configuration, the shape of the gizzard and enteric valve armature, as described in
136 Romero Arias *et al.* (2020). The taxon sampling attempted to maximize the number of species and their
137 geographic distribution, including samples of *Astalotermes* and *Anoplotermes* groups in addition to new
138 morphologically-characterized specimens. We also re-examined the voucher material of samples
139 sequenced in previous studies and whose phylogenetic position appeared inconsistent. In a few cases, we
140 found that the voucher samples contained a mixture of two species. We labelled these samples with both
141 species names. Revised species identifications are detailed in Supplementary Appendix S1 (see also Table
142 S1).

143 ***DNA extraction and sequencing***

144 Whole genomic DNA was extracted from head and thorax of three to five workers using the DNeasy
145 Blood & Tissue extraction kits (Qiagen). Because DNA extracts were sequenced at different periods of
146 time, two different approaches were used. For the first approach, the complete mitochondrial genome was
147 amplified in two long-PCR reactions with the TaKaRa LA Taq polymerase, using primers previously
148 designed for termites (Bourguignon *et al.*, 2015). The concentration of both long PCR fragments was
149 determined using a Qubit 3.0 fluorometer, and the two fragments were mixed in equimolar concentration.
150 Libraries were prepared with the NEBNext Ultra II DNA Library Prep Kit (New England Biolabs) and
151 sequenced with Illumina MiSeq. For the second approach, whole genomic DNA libraries were directly
152 prepared with the aforementioned NEB kit and sequenced using Illumina HiSeq4000.

153 ***Assembly and annotation of mitochondrial genomes***

154 Paired-end reads were quality-assessed using FastQC v0.11.7 ([http://www.bioinformatics.
155 babraham.ac.uk/projects/fastqc/](http://www.bioinformatics.babraham.ac.uk/projects/fastqc/)) and adapter sequences were removed with Trim Galore v0.4.5
156 (http://www.bioinformatics.babraham.ac.uk/projects/trim_galore/) using default settings. Mitochondrial

157 reads were identified using the mitogenome of *Astalotermes murcus* Sands (accession no. KY224676) as
158 a reference and assembled using GetOrganelle v1.5.1 (Jin *et al.*, 2020). Each resulting assembly graph
159 was inspected with Bandage v0.8.1 (Wick *et al.*, 2015) and mitochondrial genome sequences were
160 manually circularized when necessary. Control regions were discarded from the final assemblies as they
161 provide limited phylogenetic information and are difficult to accurately assemble with short reads. We
162 used the MITOS2 Webserver with the invertebrate genetic code and the protein prediction method of
163 Donath *et al.* (2019) to annotate the two rRNA genes, 22 tRNA genes, and 13 protein-coding genes. Other
164 parameters were set to default. Annotated genomes are deposited in GenBank (accession numbers in
165 Table S1). In total, we generated 67 new mitochondrial genome sequences, mostly from African species
166 (54). Fifty-nine mitochondrial genomes were complete, and eight mitochondrial genomes were nearly
167 complete because of ambiguous circularization. The mitochondrial genomes from Bourguignon *et al.*
168 (2015), which included 60 non-Apicotermitinae termites and eight non-termite polyneopteran insects,
169 were used as outgroups (Table S2). Therefore, the final data set comprised 181 mitochondrial genomes,
170 including 113 genomes of Apicotermitinae.

171 ***Sequence alignment***

172 We aligned separately each of the two rRNA genes, 22 tRNA genes, and 13 protein-coding genes using
173 MAFFT v7.300b (Katoh *et al.*, 2002; Katoh & Standley, 2013) with default settings. Protein-coding
174 genes were aligned as protein sequences and back-translated into nucleotide sequences using PAL2NAL
175 (Suyama *et al.*, 2006). rRNAs and tRNAs were aligned as DNA sequences. The 37 aligned genes were
176 concatenated and partitioned into five partitions: one for each codon position of the combined protein-
177 coding genes; one for the combined 12S and the 16S rRNA genes; and one for the combined tRNA genes.
178 We found no clear evidence of mutational saturation for the third codon positions of the protein-coding
179 genes ($I_{SS}=0.572$, $I_{SS,cSym}=0.809$) using Xia's method implemented in DAMBE (Xia *et al.*, 2003; Xia &
180 Lemey, 2009) and therefore retained the third codon positions in our phylogenetic analyses.

181 ***Phylogenetic inference***

182 We used RAxML version 8.2.4 (Stamatakis, 2014) to reconstruct a maximum-likelihood phylogenetic
183 tree, with the GTR+G model for each partition. Bootstrap values were estimated from 1000 replicates.
184 We used MrBayes version 3.2 (Ronquist *et al.*, 2012) to reconstruct a Bayesian phylogenetic tree. The
185 analysis was run with four chains (three hot and one cold), and we estimated posterior distributions using
186 Markov chain Monte Carlo (MCMC) sampling, with samples drawn every 5000 generations. The chain
187 was run for a total of 10 million generations, with the first 1 million generations discarded as burnin, as
188 suggested by inspection of the trace files using Tracer v1.5 (Rambaut & Drummond, 2009). We used a
189 GTR model with gamma-distributed rate variation across sites (GTR+G) for each partition. The analysis
190 was run in triplicate to ensure convergence of the chains and check for consistency. The effective sample
191 size was higher than 400 for every parameter of every run. Node support was estimated using Bayesian
192 posterior probabilities.

193 ***Molecular dating***

194 We estimated time-calibrated trees using BEAST2 version 2.4.4 (Bouckaert *et al.*, 2014). We performed
195 the analyses with and without third codon positions to assess the influence of third codon positions on
196 time estimates. The trees were reconstructed using an uncorrelated lognormal relaxed clock to model rate
197 variation among branches, with single model for each partition, allowing different relative rates. A Yule
198 speciation model was used as tree prior. We used a GTR+G model of nucleotide substitution for each
199 partition. The chains were run for 500 million steps and were sampled every 10,000 generations to
200 estimate the posterior distribution. We discarded the first 50 million steps as burn-in, as suggested by
201 inspection of the trace files using Tracer v1.5 (Rambaut & Drummond, 2009). We used the 13 fossils
202 used by Bucek *et al.* (2019) (see Table 1). The phylogenetic position and age of fossils were carefully
203 assessed as recommended by Parham *et al.* (2012). Bucek *et al.* (2019) provided detailed justifications
204 about the placement of these fossils, which we followed. The youngest fossil age estimates reported on
205 the Fossilworks database (Alroy, 2016) were used as minimum age constraints. We determined soft upper
206 bounds using phylogenetic bracketing (Ho & Phillips, 2009). Each calibration was implemented as an
207 exponential prior of node time. The analyses were run in triplicate to ensure convergence of the chains
208 and check for consistency.

209 ***Reconstruction of ancestral distribution***

210 The ancestral distribution of Apicotermitinae was reconstructed using the ace function of the R package
211 APE version 5.0 (Paradis & Schliep, 2018). We used the Maximum Likelihood model described by Pagel
212 (1994) for discrete data. We tested three models available in APE: the equal-rates model (ER), the all-
213 rate-different model (ARD) and the symmetrical model (SYM). The function was implemented as follow:
214 “ace(distribution, tree, type="discrete", model="ER" or "ARD" or "SYM", CI=TRUE)”. Other
215 parameters were set on default values. We also used the Bayesian Binary mcmc analysis implemented in
216 RASP4.2 (Yu *et al.*, 2015, 2020), with maximum number of areas set to 1 and 3. We ran separate
217 analyses for the four possible combinations of state frequencies, set to fixed (JC) or estimated (F81), and
218 among-site rate variation, set to equal or gamma (+G). Default values were used for other parameters.
219 The seven analyses, implemented in APE and RASP4.2, were run on the four phylogenetic trees
220 reconstructed in this study. Sampling locations were used to assign each tip to one biogeographic realm.
221 Apicotermitinae are distributed across three biogeographic realms, as described by Holt *et al.* (2013):
222 Afrotropical, Neotropical, and Oriental. We reconstructed ancestral distribution on the maximum-
223 likelihood tree, the Bayesian tree, and the two time-calibrated trees.

224 ***Reconstruction of soldier loss***

225 We used the ace function of the R package APE version 5.0 (Paradis & Schliep, 2018) to reconstruct the
226 evolution of soldier loss in Apicotermitinae. As for the reconstruction of ancestral distribution, we used

227 three models, the ER model, the ARD model and the SYM model. Soldier presence, or absence, was
228 determined for each tip of the phylogenetic trees based on literature data.

229

230 **Results**

231 *Molecular phylogeny*

232 Our phylogenetic trees fully supported the monophyly of Apicotermitinae (Figs 1 and S1-S3). African
233 soldiered taxa (the *Apicotermes*-group) formed a paraphyletic assemblage, composed of two or three
234 lineages, within which a clade composed of Asian genera and soldierless African and Neotropical taxa
235 was nested (Figs 1 and S2-S3). This latter clade was divided into four lineages, fully supported in all
236 analyses: (I) the African soldierless species, with the exclusion of *Adaiphrotermes* and *Apolemotermes*
237 **gen. n.**, were retrieved as sister to the other three lineages, (II) the Asian *Speculitermes*-group was sister
238 to the last two lineages, (III) the African genera *Adaiphrotermes* and *Apolemotermes gen. n.*, and their
239 sister group, (IV) the Neotropical soldierless *Anoplotermes*-group.

240 Discrepancies among analyses were found for the position of soldiered lineages. More precisely, the
241 position of the clade including *Koutabatermes gen. n.* + (*Hoplognathotermes* Silvestri + *Labidotermes*
242 Deligne & Pasteels) was variable among analyses (Figs 1 and S1-S3). Similarly, the position of species
243 within the *Astalotermes*-group and the *Anoplotermes*-group was variable. The relationships among taxa of
244 *Astalotermes*-group were often weakly supported, and several genera were retrieved as polyphyletic, i.e.
245 *Astalotermes*, *Anenteotermes* and *Astratotermes*. Among the monophyletic genera, we retrieved well-
246 supported sister relationships between *Acholotermes* Sands and *Amicotermes* Sands and between
247 *Ateuchotermes* and *Anaorotermes* Sands. Other well-supported monophyletic genera were *Alyscotermes*
248 Sands, *Acidnotermes* Sands, *Aderitotermes*, and *Adaiphrotermes*. Within the neotropical *Anoplotermes*-
249 group (clade IV), the relationships among genera were weakly supported, and many species, referred to as
250 *Anoplotermes*-group sp., were found on long branches and belong to undescribed genera (Figs 1 and S1-
251 S3). The genus *Ruptitermes* Mathews appeared to be polyphyletic, the arboreal *R. arboreus* Emerson
252 being broadly separated from the other species of the genus.

253 *Divergence time estimation*

254 The time-tree reconstructed with third codon positions included yielded older age estimates (Fig. S1), up
255 to 10.9 million years (My) older than the analysis with third codon positions excluded (Fig. 1). The
256 ranges given hereafter encompass the results of both analyses, with and without third codon positions. We
257 estimated that the most recent common ancestor of Apicotermitinae lived 39.5–48.6 million years ago
258 (hereafter Ma) (95% HPD: 34.7–53.2 Ma), during the middle Eocene. The most recent common ancestor
259 of the soldierless Apicotermitinae + *Speculitermes*-group was estimated at 34.9–44.2 Ma (95% HPD:
260 30.8–48.5 Ma). The split between the *Speculitermes*-group and their sister group was dated at 31.7–41.6
261 Ma (95% HPD: 27.7–45.9 Ma), during the early Oligocene. The Neotropical *Anoplotermes*-group
262 diverged from its African sister lineage (*Adaiphrotermes* + *Apolemotermes gen. n.*) 28.0–38.0 Ma (95%

263 HPD: 24.4–42.0 Ma). The age estimates of cladogenesis for the current taxonomic groups are
264 summarized in Table 2.

265 ***Ancestral distribution***

266 We reconstructed the ancestral distribution of Apicotermitinae on the four phylogenetic trees generated in
267 this study. For each tree, we tested three Maximum Likelihood models and four Bayesian Binary mcmc
268 models. Bayesian models allowing multiple distribution areas yielded similar trends on ancestral
269 distribution. Therefore, the results were congruent among analyses, and consequently, we only present
270 here the results of the ER model that posits an equal rate of transition among states (Figs S4-S7). Our
271 results indicate that the Apicotermitinae originated in the African realm, and dispersed from there twice:
272 once to the Oriental realm, where they gave rise to the *Speculitermes*-group, and once to the Neotropical
273 realm, where they gave rise to the *Anoplotermes*-group.

274 ***Reconstruction of soldier loss***

275 We reconstructed the evolution of soldier loss in Apicotermitinae on the four phylogenetic trees generated
276 in this study using three Maximum Likelihood models. The reconstructions of the four phylogenetic trees
277 yielded almost identical results and therefore we only present here the results of the reconstructions on the
278 phylogenetic tree reconstructed with MrBayes. The ARD model clearly supported independent loss of
279 soldiers in the African soldierless Apicotermitinae and in the Neotropical soldierless *Anoplotermes*-group
280 (Fig. S8). In contrast, the ER model and the SYM model provided more ambiguous results, with the
281 scenario of a dual loss of soldiers in the African soldierless Apicotermitinae and in the Neotropical
282 soldierless *Anoplotermes*-group being equally probable to another scenario implying a loss of soldiers in
283 the ancestor of non-*Apicotermes*-group Apicotermitinae followed by a secondary reacquisition of soldiers
284 in the *Speculitermes*-group (Figs S9-10).

285 ***Taxonomy***

286 **Apicotermitinae Grassé and Noirot, 1955**

287 Type genus: *Apicotermes* Holmgren, 1912

288 ***Koutabatermes* Romero Arias & Roisin, gen. n.**

289 <http://zoobank.org/urn:lsid:zoobank.org:act:EB5EED27-355F-40F5-9FAD-D7C812466395>.

290 (Figs 2, 3, 4A)

291 Type species: *Koutabatermes spinifer* Romero Arias & Roisin, **sp. n.**, described below. This
292 genus is presently monotypic.

293 *Diagnosis.* The general configuration of the worker digestive tube (Fig. 2), characterized by the
294 absence of a mixed segment and a rather short P1, matches that of other genera of the *Apicotermes*-group
295 (Noirot, 2001). *Koutabatermes* workers possess a singular enteric valve armature, comprising six

296 subequal membraneous cushions covered with polygonal scales in their basal part, bearing numerous tiny
297 spines in their middle part, and distally dome-shaped, bearing a variable number (5-25) of sharp spines
298 about 20 μm in length, penetrating into the valve seating (Fig. 3C,D). Species of the *Labidotermes*
299 subgroup (see Noirot, 2001) also possess six subequal scaly cushions, but they bear a stout spine basally
300 and no apical armature entering the paunch. In the clade comprising *Apicotermes* and *Coxotermes*, the
301 armature is always heavily asymmetrically sclerotized in its apical part and of very diverse shape
302 resembling spiny, club- or feather-shaped expansions, as it enters the paunch. *Eburnitermes* and
303 *Machadotermes* possess elongated spiny pads internally, prolonged in the seating by long plates bearing
304 spines or pectinated scales. In *Phoxotermes*, *Jugositermes* and *Trichotermes*, the apical part of the pads is
305 heavily sclerotized and bears spines of various shapes.

306 *Description.*

307 Imago. Unknown.

308 Soldier. Unknown, but the phylogenetic position of *Koutabatermes* among soldiered taxa suggests that
309 this caste may exist.

310 Worker. Head, thorax, abdomen and legs covered with numerous setae. Antennae with 14 articles.
311 Postclypeus moderately inflated. Fore coxa without prominent ridge or projection, fore tibia slender, not
312 inflated. Tibial spurs 3, 2, 2. Crop voluminous, gizzard armature reduced to six pulvilli, one of them (in
313 position 4 according to Romero Arias *et al.*, 2020) much larger than the other five. All pulvilli bear a
314 group of 25-50 pointed spines, about 10 μm long (Fig. 3A,B). Mesenteron forming almost complete loop;
315 M–P1 junction circular, without mixed segment; P1 short, about 3 times as long as wide (Fig. 2). Enteric
316 valve armature comprising six subequal bulky membraneous cushions within lumen of P2, extending
317 distally to emerge within P3, where each cushion is capped by irregularly-oriented curved spines in
318 variable number (5–25), about 20 μm long. No distinct lobes at P2–P3 junction. First section of the
319 paunch slightly narrower and about half the length of P1, internally-garnished with tiny spicules but
320 without conspicuous sclerotized armature as present in *Gastrotermes* (Scheffrahn, 2020).

321 *Etymology.* From Koutaba, a town in Cameroon, and Latin *termes*, termite. Gender: masculine.

322 ***Koutabatermes spinifer* Romero Arias and Roisin, sp. n.**

323 <http://zoobank.org/urn:lsid:zoobank.org:act:46DC8A42-06E0-47B7-86F4-27BA95970EB7>.

324 (Figs 2, 3, 4A)

325 *Type material.* Holotype: worker. Paratypes: workers, from the same series (most probably from
326 the same colony) as the holotype. The whole series comprises about 60 workers. Cameroon, Région
327 Ouest, near the town of Koutaba, Koumaja village (N 05.6244°, E 10.7542°), elevation (GPS) 1203 m,
328 collected on 29 May 2017. Collected in soil under an old nest of *Pseudacanthotermes* sp. at the edge of a
329 cultivated field (J. Romero Arias, Y. Roisin, accession CMRT074).

330 *Type repository.* AfricaMuseum (formerly known as Royal Museum of Central Africa), Tervuren,
331 Belgium. Part of the type series is stored in the ULB (Université Libre de Bruxelles) collection.

332 *Diagnosis.* As for the genus (*vide supra*).

333 *Description.*

334 Worker. Monomorphic, rather large for the subfamily. Head, thorax, abdomen and legs covered with
335 numerous, rather long (13–20 μm) setae. Head capsule and antennae pale brownish-yellow, remainder of
336 the body whitish. Fore tibia with three spurs, the external one about half the length of the other two. Left
337 mandible with posterior edge of apical tooth about 1.5 times as long as anterior edge of first marginal
338 tooth; premolar tooth (as per Deligne, 1999; "subsidiary marginal" of Sands, 1972) as long as third
339 marginal, visible in front of molar prominence (Fig. 4A). Right mandible with posterior edge of apical
340 tooth about 1.8 times as long as anterior edge of first marginal (Fig. 4A).

341 Measurements (in mm) of 10 workers: mean (range), holotype.

342 Head length to front margin of postclypeus: 1.216 (1.176–1.275), 1.218; postclypeus length: 0.312
343 (0.291–0.336), 0.294; head maximum width: 1.323 (1.277–1.359), 1.344; pronotum maximum width:
344 0.852 (0.830–0.883), 0.852; fore tibia length: 1.003 (0.968–1.040), 1.023; fore tibia width: 0.137 (0.121–
345 0.151), 0.126; hind tibia length: 1.392 (1.366–1.423), 1.396; fore tibia length/width ratio: 7.343 (6.628–
346 8.125), 8.119.

347 Measurements (in mm) of mandibles from 5 workers: mean (range).

348 Left mandible. Apical tooth to first marginal (L_A in Sands, 1972): 0.147 (0.143–0.155); first to third
349 marginal (L_1): 0.190 (0.185–0.195); third marginal to molar (L_m): 0.061 (0.054–0.069). Right mandible.
350 Apical to first marginal (R_A): 0.155 (0.148–0.177); first to second marginal (R_1): 0.125 (0.120–0.128);
351 second marginal to molar (R_m): 0.083 (0.076–0.088).

352 This species was called "Cameroon Genus C" in Romero Arias *et al.* (2020), and illustrated in Figs A7C
353 (gizzard and enteric valve) and A8C (gizzard).

354 *Etymology:* Latin *spinifer*, bearing spines, referring to the enteric valve armature of the worker.

355

356 **Genus *Apolemotermes* Romero Arias & Roisin, gen. n.**

357 <http://zoobank.org/urn:lsid:zoobank.org:act:4747BA58-8470-42CB-8209-87CDE0F050E9>.

358 (Figs 4B,C, 5, 6)

359 Type species: *Apolemotermes fodiens* Romero Arias & Roisin, **sp. n.**, described below. This
360 genus is presently monotypic.

361 *Diagnosis.* The general configuration of the worker digestive tube (Fig. 5), characterized by a
362 mixed segment with the mesenteric part on the inner side of the gut loop and a long P1, corresponds to the
363 usual pattern of soldierless Apicotermitinae. The mixed segment is rather long, about twice the width of
364 the mesenteron, slightly thickened but without distinct bulge at the end of its mesenteric part. The gizzard
365 features five weakly developed pulvilli (Fig. 6A). The enteric valve armature comprises six subequal
366 broadly reticulated pads with almost parallel sides, ending rather abruptly at the entrance of P3. They
367 show a faint crescent-shaped thickening at their base (Fig. 6B).

368 *Adaiphrotermes* species also possess an elongated mixed segment, but it terminates in a distinct
369 mesenteric bulge (Sands, 1972). Pulvilli of the gizzard are more prominent in *Adaiphrotermes* species and
370 bear distinct pectinated scales (Fig. 7A). The enteric valve armature of *Adaiphrotermes* species (Figs
371 7B,C) consists of parallel pads extending through the length of the narrow tubular section of P2, variable
372 according to the species. As in *Apoletotermes* **gen. n.**, their distal end is almost straight, rectangular.
373 Pads are covered with imbricated (fish-like) scales, more prominent basally.

374 *Anenteotermes* and *Aderitotermes* are the other African genera possessing a long mixed segment (Sands,
375 1972). *Anenteotermes* comprises some tiny species with enteric valve armatures harbouring very
376 distinctive sclerotized ornamentations (Sands, 1972; Scheffrahn & Roisin, 2018). Other species possess
377 scaly pads, with an ovoid or fusiform shape (not distally rectangular). *Aderitotermes* includes much larger
378 species, with distinctive enteric valves (Sands, 1972).

379 Among African Apicotermitinae, *Adaiphrotermes* and *Apoletotermes* **gen. n.** stand out for their highly
380 inflated fore tibiae, but *Apoletotermes* **gen. n.** (Fig. 4C), with a length/width ratio below 3, appears more
381 extreme than *Adaiphrotermes* in this respect.

382 *Description.*

383 Imago. Unknown.

384 Soldier. Unknown. *Apoletotermes* **gen. n.** is the sister genus of *Adaiphrotermes*. Together, they form the
385 sister group of the Neotropical Apicotermitinae, all of which are soldierless, strongly suggesting that
386 soldiers are absent.

387 Worker. Head and body covered by numerous short, erect setae. Antennae with 14 articles. Postclypeus
388 only slightly raised, in line with frons. Fore coxa without prominent ridge or projection, fore tibia
389 strongly inflated (Fig. 4C). Tibial spurs 2, 2, 2. Crop moderately developed, gizzard armature reduced to
390 five weakly raised pulvilli bearing only a faint projection (Fig. 6A). Mesenteron forming almost complete
391 loop; distinct mixed segment, about as long as twice the mesenteric diameter. Mesenteric part of mixed
392 segment slightly enlarged distally, but not forming a distinct terminal bulge as found in *Adaiphrotermes*
393 species (Sands, 1972). P1 long and of constant diameter, enteric valve situated on the right side at the
394 back of the paunch. Enteric valve seating without distinct lobes. Enteric valve armature comprising six
395 subequal, reticulated pads, with a small thickening at their base (Fig. 6B).

396 *Etymology.* Ancient Greek ἀπόλεμος, peaceful, and Latin *termes*, termite. This name evokes the
397 absence of soldiers, in the line of names created by Sands (1972) for 16 new African soldierless genera.
398 Gender: masculine.

399 ***Apolemotermes fodiens* Romero Arias & Roisin, sp. n.**

400 <http://zoobank.org/urn:lsid:zoobank.org:act:3001D19F-6EB8-410F-9287-F7BC7C6026B8>.

401 (Figs 4B,C, 5, 6)

402 *Type material.* Holotype: worker. Paratypes: workers, from the same series (most probably from
403 the same colony) as the holotype. Whole series comprises about 60 workers. Cameroon, Région Centre,
404 near town of Mbalmayo, Feikele village (N 03.4807°, E 11.5772°), elevation (GPS) 688 m, 06 June 2017.
405 Collected in soil in forest fragment (J. Romero Arias, Y. Roisin, accession CMRT159).

406 *Type repository.* AfricaMuseum, Tervuren, Belgium. Part of the type series in the ULB
407 collection.

408 *Diagnosis.* As for the genus (*vide supra*).

409 *Description.*

410 Imago. Unknown.

411 Soldier. Unknown and probably absent.

412 Worker. Monomorphic, very small, with elongated body. Head and body covered by numerous short,
413 erect setae, about 0.04 mm long. Head capsule pale yellow, remainder of the body and appendages
414 whitish. Fore tibia with two developed spurs, external one vestigial. Enteric valve pads subequal—the
415 shortest ones about $\frac{3}{4}$ the length of the longest ones—with almost parallel sides, distal edge slightly
416 convex. Pads broadly reticulated, with faint crescent-shaped thickening at base, more visible on shortest
417 pads (Fig. 6B). Left mandible with posterior edge of apical tooth about 1.6 times as long as anterior edge
418 of first marginal; premolar tooth clearly shorter than third marginal, under edge of molar prominence.
419 Right mandible with posterior edge of apical tooth about twice as long as anterior edge of first marginal
420 (Fig. 4B).

421 Measurements (in mm) of 10 workers: mean (range), holotype.

422 Head length to front margin of postclypeus: 0.498 (0.474–0.519), 0.482; postclypeus length: 0.135
423 (0.121–0.151), 0.135; head maximum width: 0.506 (0.496–0.519), 0.501; pronotum maximum width:
424 0.308 (0.296–0.320), 0.299; fore tibia length: 0.359 (0.346–0.373), 0.351; fore tibia width: 0.138 (0.128–
425 0.145), 0.140; hind tibia length: 0.364 (0.346–0.380), 0.360; fore tibia length/width ratio: 2.604 (2.483–
426 2.710), 2.507.

427 Measurements (in mm) of mandibles from 5 workers: mean (range).

428 Left mandible. Apical tooth to first marginal (L_A in Sands, 1972): 0.044 (0.042–0.046); first to third
429 marginal (L_1): 0.085 (0.084–0.086); third marginal to molar (L_m): 0.026 (0.024–0.027). Right mandible.
430 Apical to first marginal (R_A): 0.046 (0.042–0.049); first to second marginal (R_1): 0.062 (0.060–0.066);
431 second marginal to molar (R_m): 0.042 (0.040–0.043).

432 *Etymology.* Latin *fodiens*, digging.

433

434 **Discussion**

435 *Phylogenetic relationships and systematics*

436 Our findings are in partial agreement with those of Inward *et al.* (2007) and Bourguignon *et al.* (2017).
437 For instance, we confirm the paraphyly of the *Apicotermes*-group, which is composed of several basal
438 lineages, closely matching the subgroups proposed by Noirot (2001) on the basis of digestive anatomy:
439 the *Labidotermes* subgroup, also comprising *Hoplognathotermes* (+ *Acutidentitermes* Emerson, not
440 sequenced), is characterized by a simple enteric valve armature wholly enclosed within the P2 section of
441 the hindgut, which probably represents an ancestral condition; the *Apicotermes* subgroup, including also
442 *Allognathotermes* Silvestri + *Duplidentitermes* Emerson and *Coxotermes* Grassé & Noirot + *Heimitermes*
443 Grassé & Noirot, possesses very sophisticated enteric valve armatures protruding into the paunch; and the
444 *Trichotermes* subgroup, including *Jugositermes* Emerson and *Phoxotermes* Collins (+ *Rostrotermes*
445 Grassé, not sequenced), displays an enteric valve with six sclerotized plates bearing numerous, variously
446 developed spines, which also penetrate into the paunch. Noirot (2001) made a fourth subgroup for
447 *Eburnitermes* Noirot and *Machadotermes* Weidner, which were not sequenced in this study. These two
448 genera possibly constitute another basal lineage. Finally, some new taxa are known from the worker only,
449 although their anatomy places them in the *Apicotermes*-group: this is the case of the new *Koutabatermes*
450 **gen. n.**, whose mitochondrial genome confirmed distant affinities with *Labidotermes* and
451 *Hoplognathotermes*. Another such taxon is the new genus labelled "*Kaktotermes*" (*nomen nudum*) by
452 Donovan (2002), which still awaits sequencing.

453 The phylogeny of Inward *et al.* (2007) featured a large clade comprising, on the one hand, the
454 *Astalotermes*-group (including all African soldierless taxa except *Adaiphrotermes*, without deeper
455 resolution), and on the other hand, an unresolved clade including *Adaiphrotermes*, which appeared
456 paraphyletic, the Asian taxa (with soldiers known in all genera, but often very rare) and the Neotropical
457 taxa (all soldierless, not further resolved). Here, we confirm the monophyly of the *Astalotermes*-group
458 and determine its sister clade with a strong support: Asian genera (*Indotermes* + *Euhamitermes*
459 Holmgren) now branch out first, as sister group to a soldierless clade including the Neotropical taxa,
460 confirmed as monophyletic (= the *Anoplotermes*-group clade), and an African branch composed of
461 *Adaiphrotermes* plus a distinctive new African genus here called *Apoletotermes* **gen. n.**
462 (*Adaiphrotermes*-group clade).

463 Inward *et al.* (2007) suggested that the loss of the soldier caste occurred only once in the evolution of the
464 Apicotermitinae, but in view of the best supported phylogeny, this hypothesis cannot account for the
465 presence of soldiers in Asian taxa. Unless soldiers have been reacquired in Asian taxa, their loss must
466 have occurred at least twice: once at the origin of the *Astalotermes*-group (clade I on Fig. 1), and once at
467 the origin of the clade composed of the *Adaiphrotermes*-group and the *Anoplotermes*-group (clades
468 III+IV on Fig. 1). The rarity of soldiers in species of the *Speculitermes*-group suggests that soldier
469 abundance gradually dwindled to the point of disappearing completely in some species of the
470 *Speculitermes*-group. We posit that a similar scenario likely took place in the ancestor of the
471 *Astalotermes*-group and in the ancestor of *Adaiphrotermes*-group + *Anoplotermes*-group. Future
472 phylogenetic trees, inferred from more comprehensive sampling, might also uncover additional loss
473 events. For example, according to Noirot (2001), the soldiered genus *Firmitermes* possesses a digestive
474 anatomy reminiscent of soldierless species, and the soldierless genus *Skatitermes* anatomically matches
475 the *Apicotermes*-group, raising the possibility of additional soldier losses not represented in our
476 phylogenetic reconstructions.

477 Thus far, most generic descriptions of Apicotermitinae have been written in the absence of a solid
478 phylogenetic background. For instance, as Sands (1972: 51) himself admitted, *Astalotermes* was difficult
479 to define because this genus "occupies a transitional position between others with more primitive and
480 more specialized characters". Unsurprisingly, this genus came out of our study as polyphyletic. Likewise,
481 *Astratotermes*, which differs from *Astalotermes* by the enteric valve scales ending in tiny points, was
482 defined based on characters of poor phylogenetic significance and is polyphyletic. The situation is even
483 more accentuated in the Neotropics, where the genus *Anoplotermes* lumps all soldierless species that have
484 not been considered distinctive enough to deserve a transfer to another genus. All those genera are now in
485 need of an in-depth revision. The present phylogeny will constitute a useful framework to revise the
486 whole subfamily and identify characters of phylogenetic interest.

487 This work also yielded less intuitive results. For instance, the tiny *Anenteotermes nanus* Sjöstedt now
488 appears distant from the equally tiny *An. polyscolus* Sands and other species with a bilateral enteric valve
489 armature —*An. cnaphorus* Sands, *An. sp. A* (CIVT120), and probably *An. cherubimi* Scheffrahn, recently
490 described (Scheffrahn & Roisin, 2018) and awaiting sequencing. In the Neotropics, the arboreal open-air
491 forager *Ruptitermes arboreus* was known to be slightly different, on anatomical grounds, from other
492 species of the genus which are ground-dwelling litter feeders (Acioli & Constantino, 2015). Our results
493 now show that *R. arboreus* has been wrongly assigned to *Ruptitermes*, being closer to *Tetimatermes*
494 Fontes than to other *Ruptitermes* species.

495 ***Time frame of Apicotermitinae evolution***

496 As suggested by Inward *et al.* (2007) and Bourguignon *et al.* (2017), our results support the African
497 origin of Apicotermitinae. The molecular dating analyses with and without third codon positions yield age
498 estimates diverging by up to 10.9 My. This difference is likely caused by the high base compositional

499 heterogeneity at third codon positions which can influence the estimation of divergence times (Zheng *et*
500 *al.*, 2011). However, time estimates of our tree with the third codon position excluded are similar to those
501 of other phylogenetic trees (Bourguignon *et al.*, 2015, 2017; Bucek *et al.*, 2019). For instance, our
502 estimation of the most recent ancestor of Apicotermitinae diverged by less than 5 My from those time-
503 trees (Bourguignon *et al.*, 2015, 2017; Bucek *et al.*, 2019). According to both molecular clocks,
504 Apicotermitinae cladogenesis was initiated during the Eocene 39.5–48.6 Ma (95% HPD: 34.7–53.2 Ma)
505 when rainforests were more widely distributed than nowadays. Nevertheless, most clades originated after
506 the Eocene-Oligocene transition (about 34 Ma), coinciding with sharp drops in atmospheric concentration
507 of carbon dioxide (Pagani *et al.*, 2005) and global temperatures, and with retraction of the megathermal
508 rainforests to low latitudes (Morley, 2011). Thus, there is the possibility that climate cooling led to
509 species extinctions and created refuges in relicts of equatorial forests that could have driven speciation
510 events. The age estimates of our molecular clock analysis without the third codon positions match with
511 past climatic transitions and forest distributions that may have led to the diversification of the
512 Apicotermitinae lineage.

513 According to our results, migratory movements of the ancestors of the *Speculitermes* and *Anoplotermes*
514 groups occurred in two separate occasions out of the Afrotropical realm. The first dispersal event
515 occurred 21.0–31.7 Ma (95% HPD: 16.2–35.9 Ma, without 3rd codon position) or 29.6–41.6 (95% HPD:
516 23.6–45.9 Ma, with 3rd codon position) and gave rise to the Oriental soldiered species while the sister
517 lineage remained in the Afrotropical realm. The second dispersal event occurred 24.0–28.1 Ma (95%
518 HPD: 20.8–31.9 Ma, without 3rd codon position) or 34.2–38.0 (95% HPD: 30.8–41.9 Ma, with 3rd codon
519 position) and gave rise to the Neotropical *Anoplotermes* soldierless species, sister of the African
520 *Adaiphrotermes*-group. The timing of these dispersal events coincides with a generalized trend of species
521 dispersion and diversification in other insects and plants following the extensive extinction during the
522 Eocene–Oligocene transition (Maley, 1996; Engel, 2001; Morley, 2011). As suggested by Bourguignon *et*
523 *al.* (2015), we confirm the single dispersion to the Neotropical region. Since no land connection between
524 the Neotropics and the Afrotropics existed during the Tertiary, the ancestor of the *Anoplotermes*-group
525 must have reached the Neotropics over the ocean, possibly by rafting in wood (Bourguignon *et al.*, 2017).
526 However, soil-feeding behavior was recently suggested as the ancestral state in the major clade of
527 Termitidae, after the Macrotermitinae and Sphaerotermitinae branched off (Bucek *et al.*, 2019), and
528 certainly at the origin of the Apicotermitinae. Soil-feeding termites are especially poor dispersers, but a
529 possible explanation for their overseas dispersal is through nests attached to floating logs (Bourguignon *et*
530 *al.*, 2017). Another possibility is the colonization by a soil-wood interface feeder settled in a decayed part
531 of a log. The closest African living relative of the Neotropical *Anoplotermes*-group, the *Adaiphrotermes*-
532 group, is not known to build cohesive nests, but *Adaiphrotermes* species have been found on wood baits
533 (Sands, 1972). Nowadays, several neotropical species are known to build nests, often attached to tree
534 trunks or roots, and some commonly occur under bark or in decayed logs (Bourguignon *et al.*, 2016b).

535 The large number of species used in this study sheds new light on the evolution of a poorly-known
536 lineage, the Apicotermitinae, and highlights the need for efficient taxon sampling. Recently, many new
537 species of Apicotermitinae have been described, in particular in the Neotropics. However, the systematics
538 of this termite group requires an integrative approach combining morphological taxonomy and modern
539 molecular techniques. In this study, we followed an integrative taxonomic approach to describe
540 *Apolemotermes* **gen. n.** and *Koutabatermes* **gen. n.** and provide a comprehensive phylogenetic tree that
541 will make future species descriptions easier. However, a denser sampling of individual subclades in
542 *Astalotermes* and *Anoplotermes* groups is necessary to resolve intra-group relationships and understand
543 their diversification processes.

544

545

546 **Acknowledgements**

547 We thank J. Migliore for fruitful discussions about sequence alignment methods. We are grateful to K.
548 Dosso, T. Coulibaly and C.S. Tra Bi for their help during fieldwork in Ivory Coast and also to the people
549 of Ebogo II village for their kind company and support during sample collection in Cameroon. We thank
550 Régis Vigouroux and the staff of the Laboratoire Environnement for receiving us at the HYDRECO
551 research station (Petit Saut, French Guiana) during fieldwork. We also acknowledge M.C. Godoy for
552 providing a neotropical sample from Argentina. S. Chérasse helped editing the language of early drafts.
553 We thank the OIST sequencing section for assistance with DNA sequencing. This work was supported by
554 a grant from the Belgian National Fund for Scientific Research F.R.S.-FNRS (PDR T.0065.15) to YR, a
555 grant from the Van Buuren and Jaumotte–Demoulin fund to JRA, by subsidiary funding to OIST, and by
556 the Internal Grant Agency of the Faculty of Tropical Agrisciences CULS (20205014). The authors declare
557 that there are no conflicts of interest.

558

559 **Author contributions**

560 **Johanna Romero Arias:** Conceptualization, Data curation, Formal analysis, Funding acquisition,
561 Investigation, Methodology, Validation, Visualization, Writing-original draft, Writing-review & editing.
562 **Arthur Boom:** Data curation, Formal analysis, Methodology, Validation, Writing-original draft.
563 **Menglin Wang:** Data curation, Investigation. **Crystal Clitheroe:** Investigation. **Jan Šobotník:**
564 Resources. **Petr Stiblik:** Resources. **Thomas Bourguignon:** Conceptualization, Data curation, Formal
565 analysis, Funding acquisition, Methodology, Resources, Writing-original draft, Writing - review &
566 editing. **Yves Roisin:** Conceptualization, Data curation, Funding acquisition, Resources, Writing-original
567 draft, Writing-review & editing, Supervision.

568

569 **References**

- 570 Acioli, A.N.S. & Constantino, R. (2015) A taxonomic revision of the neotropical termite genus
571 *Ruptitermes* (Isoptera, Termitidae, Apicotermitinae). *Zootaxa*, **4032**, 451–492.
- 572 Ahmad, M. (1963) On the phylogenetic position of *Indotermes*, with description of a new species
573 (Isoptera, Termitidae). *Annals and Magazine of Natural History (Series 13)*, **6**, 395–399.
- 574 Alroy, J. (2016) Fossilworks: Gateway to the Paleobiology Database. Available from:
575 <http://fossilworks.org/> (Accessed May 2020).
- 576 Bouckaert, R., Heled, J., Kühnert, D., Vaughan, T., Wu, C-H., Xie, D., Suchard, M.A., Rambaut, A. &
577 Drummond, A.J. (2014) BEAST 2: A Software platform for Bayesian evolutionary analysis.
578 *PLOS Computational Biology*, **10**, e1003537.
- 579 Bourguignon, T., Leponce, M. & Roisin, Y. (2011) Beta-diversity of termite assemblages among primary
580 French Guiana rain forests. *Biotropica*, **43**, 473–479.
- 581 Bourguignon, T., Lo, N., Cameron, S.L., Šobotník, J., Hayashi, Y., Shigenobu, S., Watanabe, D., Roisin,
582 Y., Miura, T. & Evans, T.A. (2015) The evolutionary history of termites as inferred from 66
583 mitochondrial genomes. *Molecular Biology and Evolution*, **32**, 406–421.
- 584 Bourguignon, T., Lo, N., Šobotník, J., Ho, S.Y.W., Iqbal, N., Coissac, É., Lee, M., Jendryka, M.M.,
585 Sillam-Dussès, D., Křížková, B., Roisin, Y. & Evans, T.A. (2017) Mitochondrial phylogenomics
586 resolves the global spread of higher termites, ecosystem engineers of the tropics. *Molecular*
587 *Biology and Evolution*, **34**, 589–597.
- 588 Bourguignon, T., Scheffrahn, R.H., Krecek, J., Nagy, Z.T., Sonet, G. & Roisin, Y. (2010) Towards a
589 revision of the Neotropical soldierless termites (Isoptera: Termitidae): redescription of the genus
590 *Anoplotermes* and description of *Longustitermes*, gen. nov.*. *Invertebrate Systematics*, **24**, 357–
591 370.
- 592 Bourguignon, T., Scheffrahn, R.H., Nagy, Z.T., Sonet, G., Host, B. & Roisin, Y. (2016a) Towards a
593 revision of the Neotropical soldierless termites (Isoptera: Termitidae): redescription of the genus
594 *Grigiotermes* Mathews and description of five new genera. *Zoological Journal of the Linnean*
595 *Society*, **176**, 15–35.
- 596 Bourguignon, T., Šobotník, J., Dahlsjö, C.A.L. & Roisin, Y. (2016b) The soldierless Apicotermitinae:
597 insights into a poorly known and ecologically dominant tropical taxon. *Insectes Sociaux*, **63**, 39–
598 50.
- 599 Bucek, A., Šobotník, J., He S., Shi M., McMahon D.P., Holmes E.C., Roisin, Y., Lo, N. & Bourguignon,
600 T. (2019) Evolution of termite symbiosis informed by transcriptome-based phylogenies. *Current*
601 *Biology*, **29**, 3728–3734.
- 602 Charpentier, T. von (1843) Über einige fossile Insecten aus Radoboj in Croatien. *Novorum Actorum*
603 *Academiae Caesareae Leopoldino-Carolinae Naturae Curiosorum* **20**, 399–410, pl. XXI–XXIII.
- 604 Constantini, J.P., Carrijo, T.F., Palma-Onetto, V., Scheffrahn, R., Carnohan, L.P., Šobotník, J. &
605 Canello, E.M. (2018) *Tonsuritermes*, a new soldierless termite genus and two new species from
606 South America (Blattaria: Isoptera: Termitidae: Apicotermitinae). *Zootaxa*, **4531**, 383–394.
- 607 Constantino, R. (2020) Termite Database. University of Brasília. [http://www.termitologia.net/termite-](http://www.termitologia.net/termite-database)
608 [database](http://www.termitologia.net/termite-database) [May 20, 2020]
- 609 Dahlsjö, C.A.L., Parr, C.L., Malhi, Y., Meir, P. & Eggleton, P. (2015) Describing termite assemblage
610 structure in a Peruvian lowland tropical rain forest: a comparison of two alternative methods.
611 *Insectes Sociaux*, **62**, 141–150.
- 612 Dahlsjö, C.A.L., Valladares Romero, C.S. & Espinosa Iñiguez, C.-I. (2020) Termite diversity in Ecuador:
613 A comparison of two primary forest national parks. *Journal of Insect Science*, **20**, 4.

- 614 Davies, R.G. (2002) Feeding group responses of a Neotropical termite assemblage to rain forest
615 fragmentation. *Oecologia*, **133**, 233–242.
- 616 Deligne, J. (1999) Functional morphology and evolution of a carpenter’s plane-like tool in the mandibles
617 of termite workers (Insecta Isoptera). *Belgian Journal of Zoology*, **129**, 201–218.
- 618 Donath, A., Jühling, F., Al-Arab, M., Bernhart, S.H., Reinhardt, F., Stadler, P.F., Middendorf, M. &
619 Bernt, M. (2019) Improved annotation of protein-coding genes boundaries in metazoan
620 mitochondrial genomes. *Nucleic Acids Research*, **47**, 10543–10552.
- 621 Donovan, S.E. (2002) A morphological study of the enteric valves of the Afrotropical Apicotermatinae
622 (Isoptera: Termitidae). *Journal of Natural History*, **36**, 1823–1840.
- 623 Eggleton, P., Bignell, D.E., Sands, W.A., Waite, B., Wood, T.G. & Lawton, J.H. (1995) The species
624 richness of termites (Isoptera) under differing levels of forest disturbance in the Mbalmayo Forest
625 Reserve, southern Cameroon. *Journal of Tropical Ecology*, **11**, 85–98.
- 626 Eggleton, P., Davies, R.G., Connétable, S., Bignell, D.E. & Rouland, C. (2002) The termites of the
627 Mayombe Forest Reserve, Congo (Brazzaville): transect sampling reveals an extremely high
628 diversity of ground-nesting soil feeders. *Journal of Natural History*, **36**, 1239–1246.
- 629 Emerson, A.E. (1971) Tertiary fossil species of the Rhinotermitidae (Isoptera), phylogeny of genera, and
630 reciprocal phylogeny of associated Flagellata (Protozoa) and the Staphylinidae (Coleoptera).
631 *Bulletin of the American Museum of Natural History*, **146**, 243–304.
- 632 Engel, M.S. (2001) Monophyly and extensive extinction of advanced eusocial bees: insights from an
633 unexpected Eocene diversity. *Proceedings of the National Academy of Sciences of the United
634 States of America*, **98**, 1661–1664.
- 635 Engel, M.S., Grimaldi, D.A. & Krishna, K. (2007) A synopsis of Baltic amber termites (Isoptera).
636 *Stuttgarter Beiträge zur Naturkunde Serie B (Geologie und Paläontologie)*, **372**, 1–20.
- 637 Engel, M.S., Grimaldi, D.A., Nascimbene, P.C. & Singh, H. (2011) The termites of Early Eocene Cambay
638 amber, with the earliest record of the Termitidae (Isoptera). *ZooKeys*, **148**, 105–123.
- 639 Grassé, P.-P. & Noirot, C. (1955) *Apicotermes arquieri* (Isoptère) : ses constructions, sa biologie.
640 Considérations générales sur la sous-famille des Apicotermatinae nov. *Annales des Sciences
641 Naturelles. Zoologie et Biologie animale (11e série)*, **16**, 345–388, pl. I–V.
- 642 Ho, S.Y.W. & Phillips, M.J. (2009) Accounting for calibration uncertainty in phylogenetic estimation of
643 evolutionary divergence Times. *Systematic Biology*, **58**, 367–380.
- 644 Holt, B.G., Lessard, J.-P., Borregaard, M.K., Fritz, S.A., Araújo, M.B., Dimitrov, D., *et al.* (2013) An
645 update of Wallace’s zoogeographic regions of the world. *Science*, **339**, 74–78.
- 646 Inward, D.J.G., Vogler, A.P. & Eggleton, P. (2007) A comprehensive phylogenetic analysis of termites
647 (Isoptera) illuminates key aspects of their evolutionary biology. *Molecular Phylogenetics and
648 Evolution*, **44**, 953–967.
- 649 Jin, J.-J., Yu, W.-B., Yang, J.-B., Song, Y., dePamphilis, C.W., Yi, T.-S. & Li, D.-Z. (2020)
650 GetOrganelle: a fast and versatile toolkit for accurate *de novo* assembly of organelle genomes.
651 *Genome Biology*, **21**, 241.
- 652 Jones, D.T. & Eggleton, P. (2011) Global biogeography of termites: A compilation of sources. *Biology of
653 Termites: A Modern Synthesis* (ed. by D.E. Bignell, Y. Roisin and N. Lo), pp. 477–498. Springer,
654 Netherlands.
- 655 Katoh, K., Misawa, K., Kuma, K. & Miyata, T. (2002) MAFFT: a novel method for rapid multiple
656 sequence alignment based on fast Fourier transform. *Nucleic Acids Research*, **30**, 3059–3066.

- 657 Katoh, K. & Standley, D.M. (2013) MAFFT multiple sequence alignment software version 7:
658 Improvements in performance and usability. *Molecular Biology and Evolution*, **30**, 772–780.
- 659 Krishna, K. (1996) New fossil species of termites of the subfamily Nasutitermitinae from Dominican and
660 Mexican amber (Isoptera, Termitidae). *American Museum Novitates*, **3176**, 1–13.
- 661 Krishna, K. & Grimaldi, D.A. (2003) The first Cretaceous Rhinotermitidae (Isoptera): a new species, genus,
662 and subfamily in Burmese amber. *American Museum Novitates*, **3390**, 1–10.
- 663 Krishna, K. & Grimaldi, D.A. (2009) Diverse Rhinotermitidae and Termitidae (Isoptera) in Dominican
664 amber. *American Museum Novitates*, **3640**, 1–48.
- 665 Krishna, K., Grimaldi, D.A., Krishna, V. & Engel, M.S. (2013) Treatise on the Isoptera of the World.
666 *Bulletin of the American Museum of Natural History*, **377**, 1–2704.
- 667 Maley, J. (1996) The African rain forest – main characteristics of changes in vegetation and climate from
668 the Upper Cretaceous to the Quaternary. *Proceedings of the Royal Society of Edinburgh. Section*
669 *B. Biological Sciences*, **104**, 31–73.
- 670 Martins-Neto, R.G., Mancuso, A. & Gallego, O.F. (2005) The Triassic insect fauna from Argentina.
671 Blattoptera and Coleoptera from the Ischichuca Formation (Bermejo Basin), la Rioja Province.
672 *Ameghiniana* **42**, 705–723.
- 673 Morley, R. J. (2011) Cretaceous and Tertiary climate change and the past distribution of megathermal
674 rainforests. *Tropical rainforest responses to climatic change* (ed. by M. Bush, J. Flenley and W.
675 Gosling), pp. 1–34. Springer, Praxis Books. Springer Berlin.
- 676 Nduwarugira D., Mpawenayo B. & Roisin Y. (2017) The role of high termitaria in the composition and
677 structure of the termite assemblage in Miombo woodlands of southern Burundi. *Insect*
678 *Conservation and Diversity*, **10**, 120–128.
- 679 Noirot, C. (2001) The gut of termites (Isoptera): comparative anatomy, systematics, phylogeny. II. Higher
680 termites (Termitidae). *Annales de la Société Entomologique de France (Nouvelle Série)*, **37**, 431–
681 471.
- 682 Pagani, M., Zachos, J.C., Freeman, K.H., Tipple, B. & Bohaty, S. (2005) Marked decline in atmospheric
683 carbon dioxide concentrations during the Paleogene. *Science*, **309**, 600–603.
- 684 Pagel, M. (1994) Detecting correlated evolution on phylogenies: a general method for the comparative
685 analysis of discrete characters. *Proceedings of the Royal Society of London. Series B. Biological*
686 *Sciences*, **255**, 37–45.
- 687 Paradis, E. & Schliep, K. (2018) ape 5.0: an environment for modern phylogenetics and evolutionary
688 analyses in R. *Bioinformatics*, **35**, 526–528.
- 689 Parham, J.F., Donoghue, P.C.J., Bell, C.J., Calway, T.D., Head, J.J., Holroyd, P.A., *et al.* (2012) Best
690 practices for justifying fossil calibrations. *Systematic Biology*, **61**, 346–359.
- 691 Rambaut, A. & Drummond, A.J. (2009) Tracer v1.5. <http://tree.bio.ed.ac.uk/software/tracer/>
- 692 Roisin, Y. (2021) Apicotermitinae. *Encyclopedia of Social Insects* (ed. by C.K Starr), pp. 69–72.
693 Springer, Cham, Switzerland, doi: 10.1007/978-3-319-90306-4_113-1.
- 694 Romero Arias, J., Chevalier, C. & Roisin, Y. (2020) Anatomical specializations of the gizzard in soil-
695 feeding termites (Termitidae, Apicotermitinae): Taxonomical and functional implications.
696 *Arthropod Structure and Development*, **57**, 100942.
- 697 Ronquist, F., Teslenko, M., van der Mark, P., Ayres, D.L., Darling, A., Höhna, S., Larget, B., Liu, L.,
698 Suchard, M.A. & Huelsenbeck, J.P. (2012) MrBayes 3.2: efficient Bayesian phylogenetic
699 inference and model choice across a large model space. *Systematic Biology*, **61**, 539–542.

- 700 Roonwal, M.L. (1958) Recent work on termite research in India (1947–57). *Transactions of the Bose*
701 *Research Institute*, **22**, 77–100.
- 702 Roonwal, M.L. & Chhotani, O.B. (1966) Soldier and other castes in the termite genus *Speculitermes* and
703 the phylogeny of the *Anoplotermes*-*Speculitermes* complex. *Biologisches Zentralblatt*, **85**, 183–
704 210.
- 705 Sands, W.A. (1972) The soldierless termites of Africa (Isoptera: Termitidae). *Bulletin of the British*
706 *Museum of Natural History, Entomology*, **Supplement 18**, 1–244, 9 pls.
- 707 Sands, W.A. (1998) *The Identification of Worker Castes of Termite Genera from Soils of Africa and the*
708 *Middle East*. p. 500. CAB International, Cambridge.
- 709 Scheffrahn, R.H. (2020) *Gastrotermes spinatus* gen. n. sp. n., an African soil-feeding termite described
710 from the worker caste (Isoptera, Termitidae, Apicotermittidae). *Zootaxa*, **4789**, 291–296.
- 711 Scheffrahn, R.H. & Roisin, Y. (2018) *Anenteotermes cherubimi* sp. n., a tiny dehiscent termite from
712 Central Africa (Termitidae: Apicotermittinae). *ZooKeys*, **793**, 53–62.
- 713 Schlemmermeyer, T. & Canello, E.M. (2000) New fossil termite species: *Dolichorhinotermes*
714 *dominicanus* from Dominican amber. *Papéis Avulsos de Zoologia*, **41**, 303–311.
- 715 Snyder, T.E. (1949) Catalog of termites (Isoptera) of the world. *Smithsonian Miscellaneous Collections*
716 **112**, 1–490.
- 717 Stamatakis, A. (2014) RAxML version 8: a tool for phylogenetic analysis and post-analysis of large
718 phylogenies. *Bioinformatics*, **30**, 1312–1313.
- 719 Suyama, M., Torrents, D. & Bork, P. (2006) PAL2NAL: robust conversion of protein sequence
720 alignments into the corresponding codon alignments. *Nucleic Acids Research*, **34**, 609–612.
- 721 Vršanský, P. (2002). Origin and the early evolution of mantises. *AMBA Projekty*, **6**, 1–16.
- 722 Wick, R.R., Schultz, M.B., Zobel, J. & Holt, K.E. (2015) Bandage: interactive visualization of de novo
723 genome assemblies. *Bioinformatics*, **31**, 3350–3352.
- 724 Xia, X. & Lemey, P. (2009) Assessing substitution saturation with DAMBE. *The Phylogenetic*
725 *Handbook: A practical approach to phylogenetic analysis and hypothesis testing* (ed. by A.-M.
726 Vandamme, M. Salemi and P. Lemey), pp. 615–630. Cambridge University Press, Cambridge.
- 727 Xia, X., Xie, Z., Salemi, M., Chen, L. & Wang, Y. (2003) An index of substitution saturation and its
728 application. *Molecular Phylogenetics and Evolution*, **26**, 1–7.
- 729 Yu, Y., Blair, C., & He, X. (2020) RASP 4: ancestral state reconstruction tool for multiple genes and
730 characters. *Molecular Biology and Evolution*, **37**, 604–606.
- 731 Yu, Y., Harris, A. J., Blair, C., & He, X. (2015) RASP (Reconstruct Ancestral State in Phylogenies): a
732 tool for historical biogeography. *Molecular Phylogenetics and Evolution*, **87**, 46–49.
- 733 Zheng, Y., Peng, R., Kuro-O, M. & Zeng, X. (2011) Exploring patterns and extent of bias in estimating
734 divergence time from mitochondrial DNA sequence data in a particular lineage: a case study of
735 salamanders (Order Caudata). *Molecular Biology and Evolution*, **28**, 2521–2535.

736 Table 1. Fossils used as calibration for estimating divergence times among Apicotermittinae.

Species	Minimum age constraint (MY)	Calibration group	Soft maximum bound (97.5% probability)	Reference	Note on maximum bound
<i>Juramantis initialis</i>	145.5	Dictyoptera	315.2	Vršanský (2002)	First cockroach fossils
<i>Valditermes brenanae</i>	130	Isoptera + <i>Cryptocercus</i>	235	Krishna <i>et al.</i> (2013) and references therein	<i>Triassoblatta argentina</i> , earliest fossil of Mesoblattinidae (Martins-Neto <i>et al.</i> 2005)
<i>Archeorhinotermes rossi</i>	94.3	Kalotermitidae + Rhinotermitidae + Serriteritidae + Termitidae	235	Krishna & Grimaldi (2003).	<i>Triassoblatta argentina</i> , earliest fossil of Mesoblattinidae (Martins-Neto <i>et al.</i> 2005)
<i>Dolichorhinotermes dominicanus</i>	16	<i>Dolichorhinotermes</i> + <i>Schedorhinotermes</i>	94.3	Schlemmermeyer & Canello (2000)	Oldest fossil of Rhinotermitinae
<i>Reticulitermes antiquus</i>	33.9	<i>Reticulitermes</i> + <i>Coptotermes</i> + <i>Heterotermes</i>	94.3	Engel <i>et al.</i> (2007)	Oldest fossil of Rhinotermitinae
<i>Coptotermes sucineus</i>	16	<i>Coptotermes</i> + <i>Heterotermes</i>	33.9	Emerson (1971)	Oldest <i>Heterotermes</i> fossil
<i>Constrictotermes electroconstrictus</i>	13.8	<i>Constrictotermes</i> + <i>Caetetermes</i> + <i>Nasutitermes</i>	47.8	Krishna (1996)	Oldest fossil of Termitidae
<i>Anoplotermes sensu lato</i>	13.8	South American <i>Anoplotermes</i> -group + <i>Adaiphrotermes</i> + Genus F	47.8	Krishna & Grimaldi (2009)	Oldest fossil of Termitidae
<i>Microcerotermes insularis</i>	13.8	<i>Microcerotermes</i> + Syntermitinae	47.8	Krishna & Grimaldi (2009)	Oldest fossil of Termitidae
<i>Termes primitivus</i>	13.8	<i>Cavitermes</i> + <i>Macrognothotermes</i> + Cubitermitinae	47.8	Krishna & Grimaldi (2009)	Oldest fossil of Termitidae
<i>Nanotermes</i>	47.8	Termitidae + <i>Coptotermes</i> + <i>Heterotermes</i> + <i>Reticulitermes</i>	94.3	Engel <i>et al.</i> (2011)	Oldest fossil of Rhinotermitinae
<i>Amitermes lucidus</i>	13.8	<i>Drepanotermes</i> + <i>Sinocapritermes</i> + <i>Pericapritermes</i>	47.8	Krishna & Grimaldi (2009)	Oldest fossil of Termitidae
<i>Macrotermes pristinus</i>	16	<i>Macrotermes</i> + <i>Synacanthotermes</i> + <i>Odontotermes</i>	47.8	Charpentier (1843)	Oldest fossil of Termitidae

737

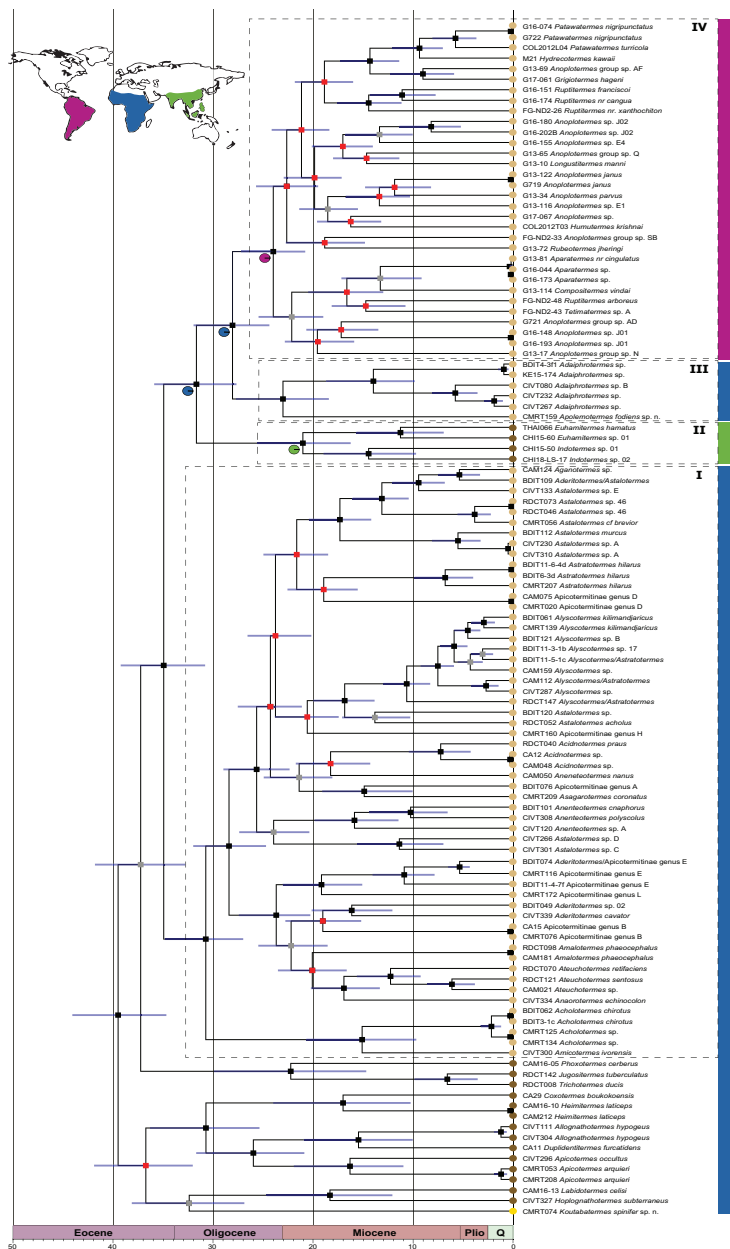
738

739
740

Table 2. Estimation dates for the major and basal Apicotermitinae clades (Ma) with all sites included and without third codon positions. The differences (δ) of node ages are included.

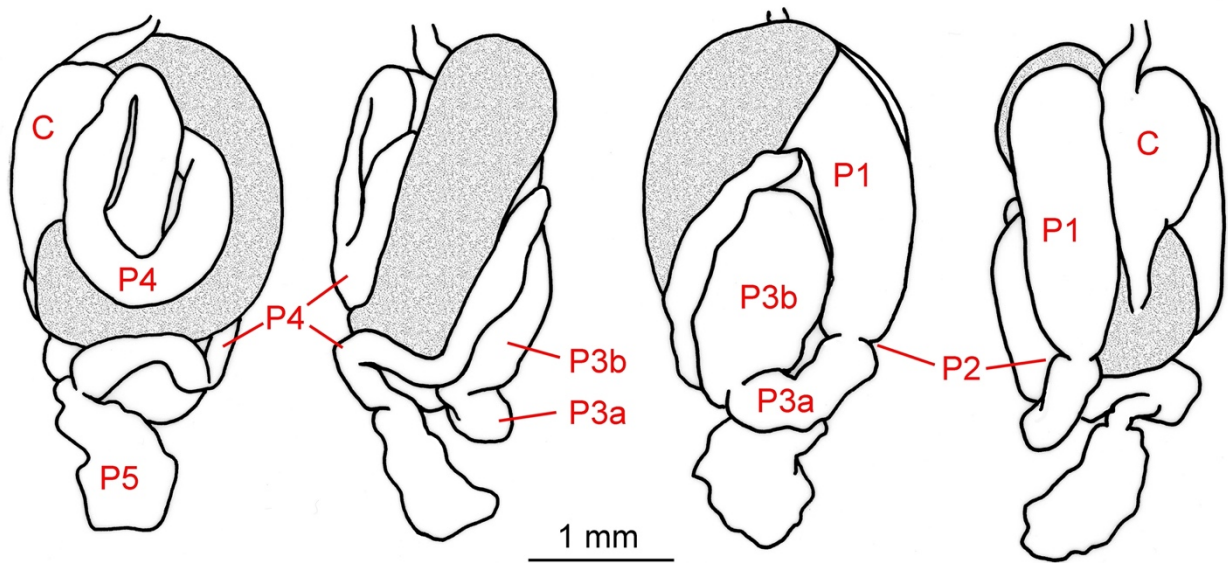
crown clade	description	without Third codon positions		with Third codon positions		δ node ages
		node ages	95% HPD	node ages	95% HPD	
I	<i>Astalotermes</i> -group	30.7	27.0-34.8	40.5	36.8-44.8	9.8
II	<i>Speculitermes</i> -group	21.0	16.2-25.6	29.6	23.6-34.8	8.6
III	<i>Adaiphrotermes</i> + <i>Apolemotermes</i> gen. n.	23.0	18.4-27.7	32.2	27.5-37.3	9.2
IV	<i>Anoplotermes</i> -group	24.0	20.8-27.2	34.2	30.8-37.9	10.2

741



742

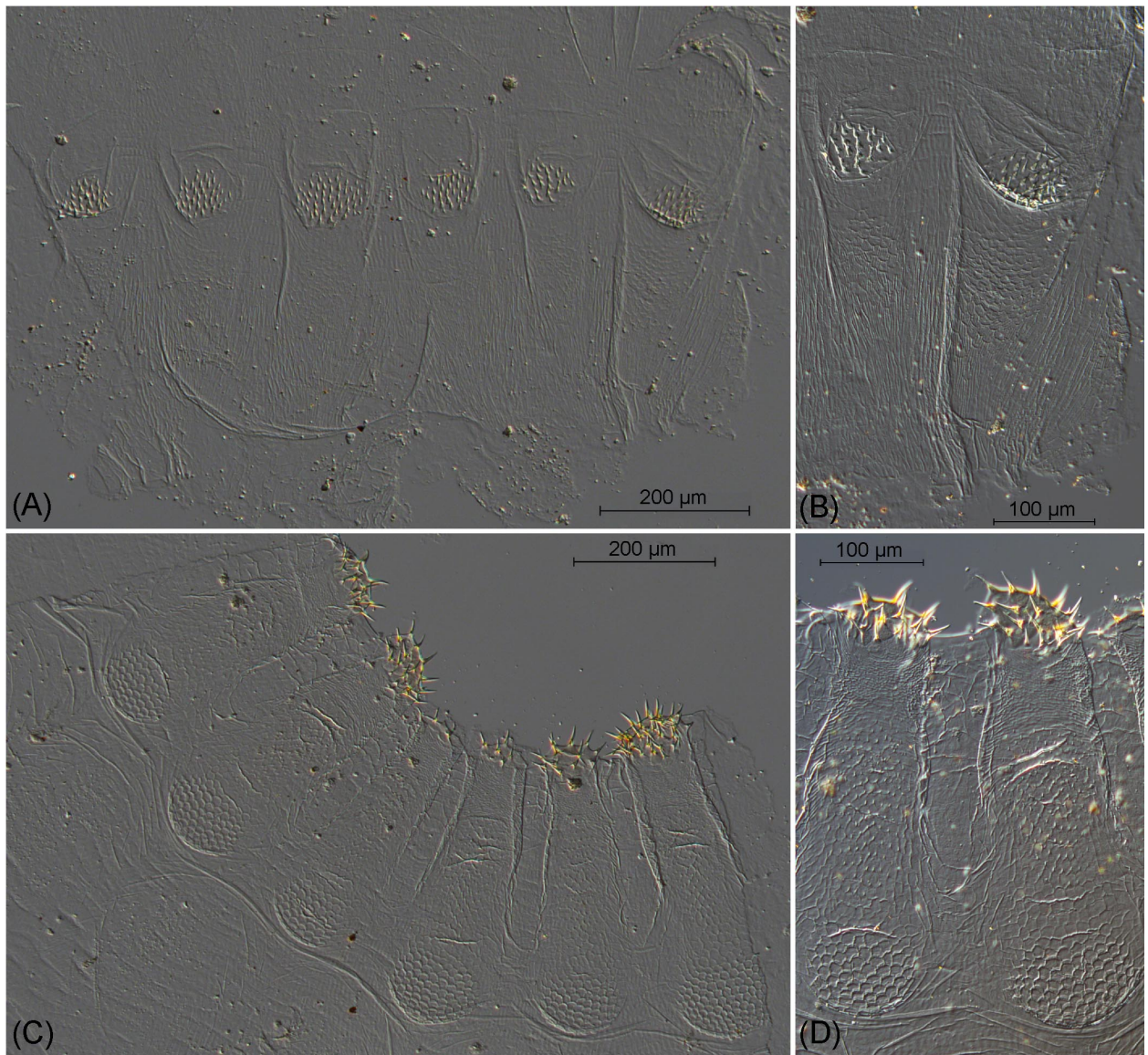
743 **Fig. 1.** Bayesian phylogenetic chronogram of Apicotermatinae inferred from mitochondrial genomes, with
 744 third codon positions excluded. The scale bar is given in millions of years. Node bars represent the 95%
 745 HPD intervals for the ages. Nodes are labelled with symbols representing posterior probabilities and
 746 bootstrap support for all analyses (1/100% = black; <1/100%= gray) and with red squares when the
 747 topology differs among analyses. Pie charts close to the nodes show the inferred relevant ancestral shifts
 748 of biogeographic distributions on the map: Afrotropical, Oriental and Neotropical realms. Wide bars
 749 indicate current distribution of species. Dotted boxes with roman numbers indicate the crown clades: I
 750 *Astalotermes*-group, II *Speculitermes*-group, III *Adaiaphrotermes* + *Apolemotermes* **gen. n.** and IV
 751 *Anoplotermes*-group. Tip circles represent soldiered (dark brown), soldierless (light brown) species and
 752 unknown soldier caste presence (yellow). Names of species include colony code and scientific name,
 753 respectively.



756

757 **Fig. 2.** Camera lucida drawings of digestive tube of *Koutabatermes spinifer* **sp. n.** worker. From left to
 758 right, viewed from above, right, below, left. Successive sections are: crop (C), mesenteron (*stippled*), first
 759 section of the paunch (P1), enteric valve (P2), third section of the paunch, subdivided into enteric valve
 760 seating (P3a) and main section (P3b), colon (P4) and rectal pouch (P5).

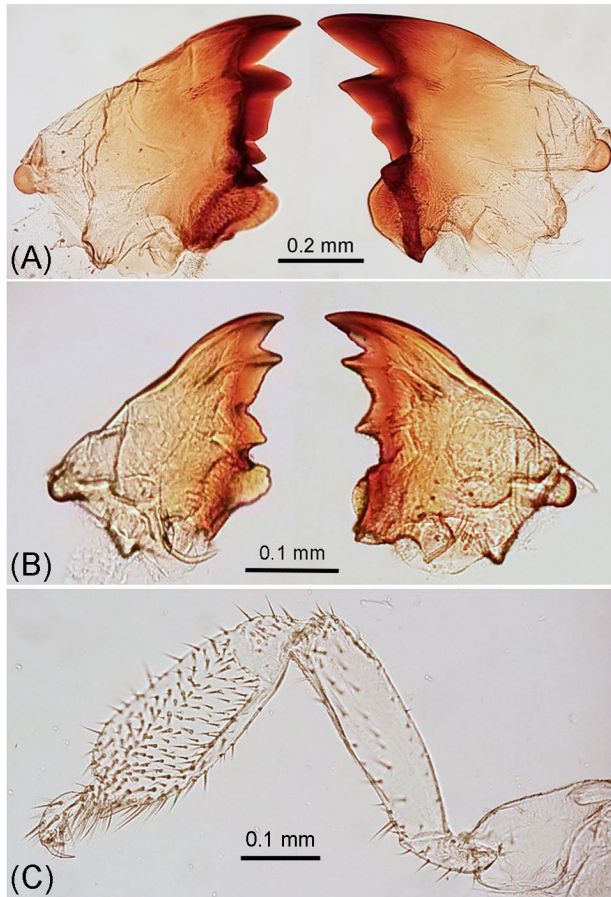
761



762

763 **Fig. 3.** Internal armature of digestive tube in worker of *Koutabatermes spinifer* sp. n. Organs splayed on
 764 slide. (A) Gizzard, showing six spiny mats corresponding to pulvilli, one of which (far right) is more
 765 developed than the others and bears tiny spicules on its upper surface. Direction of flow downwards. (B)
 766 Details of pulvilli showing scaly surface. (C) Enteric valve, showing six cushions bearing polygonal
 767 scales basally, tiny spicules in their middle part and longer, strong spines on their distal end, penetrating
 768 into the paunch. (D) Detail of two enteric valve cushions. Direction of flow upwards.

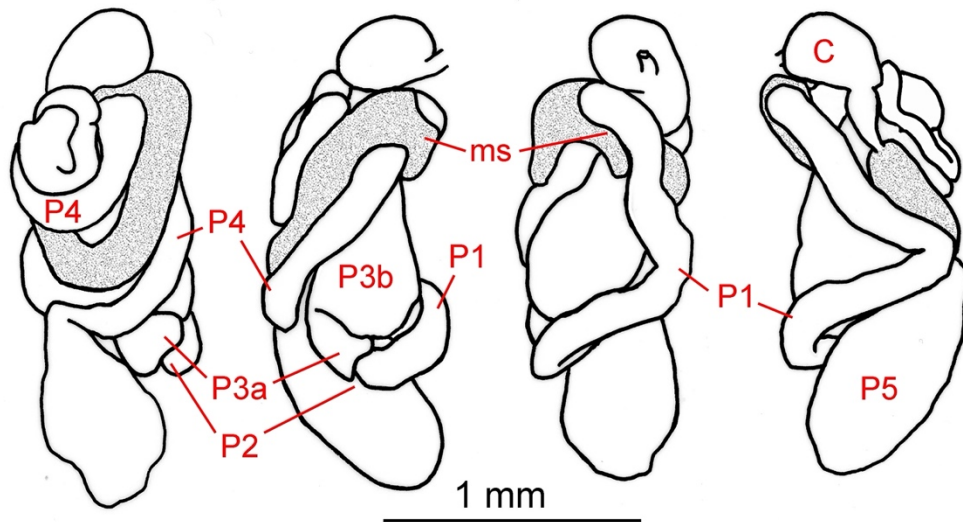
769



770

771 **Fig. 4.** Worker mandibles and fore leg. (A) Mandibles of *Koutabatermes spinifer* sp. n. (B) Mandibles of
772 *Apolemotermes fodiens* sp. n. (C) Fore leg of *Apolemotermes fodiens* sp. n., showing inflated tibia.

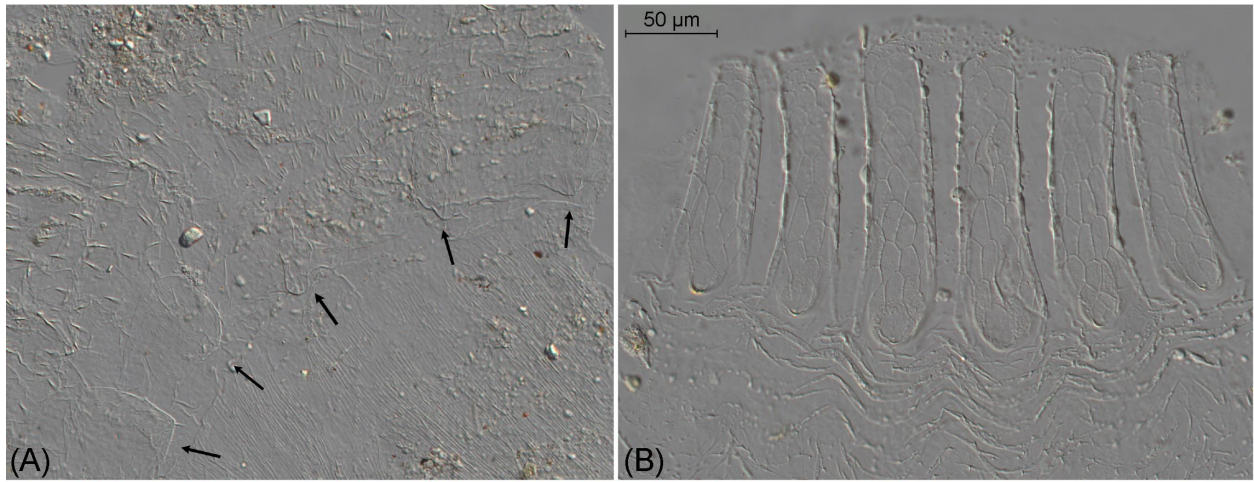
773



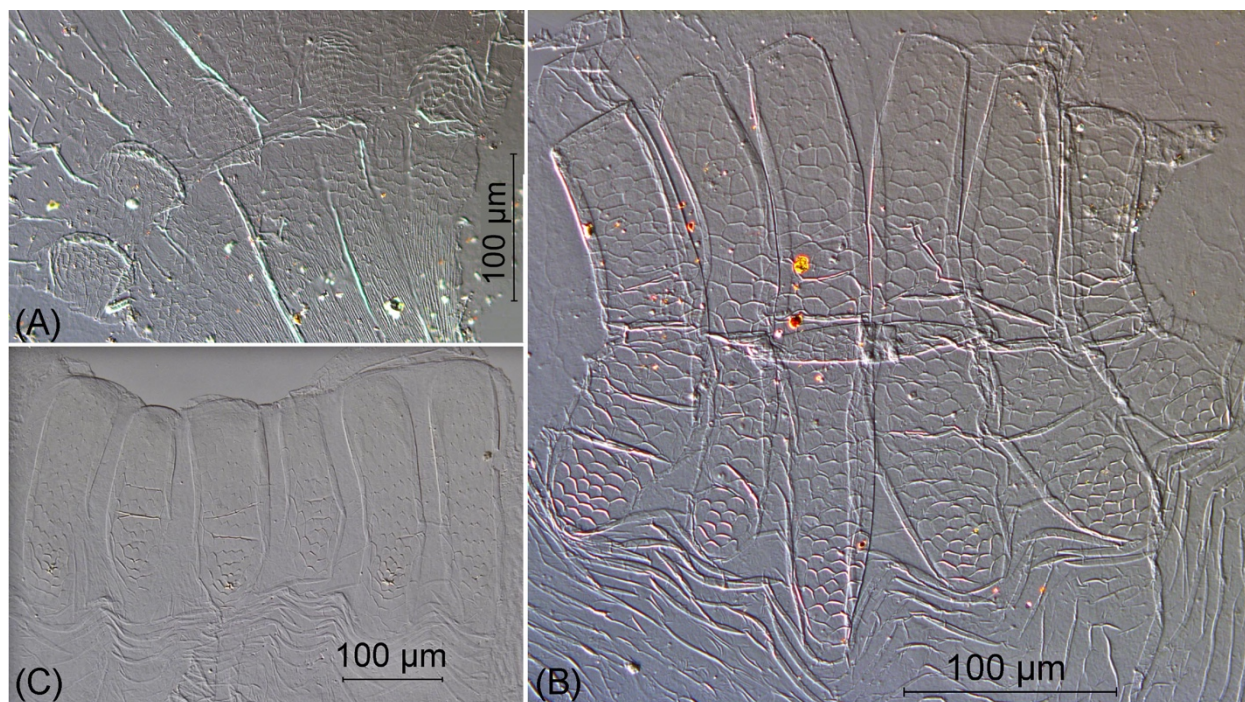
774

775 **Fig. 5.** Camera lucida drawings of digestive tube of *Apolemotermes fodiens* **sp. n.** worker. From left to
 776 right, viewed from above, right, below, left. Successive sections are: crop (C), mesenteron (*stippled*),
 777 mixed segment (ms), first section of the paunch (P1), enteric valve (P2), third section of the paunch,
 778 subdivided into enteric valve seating (P3a) and main section (P3b), colon (P4) and rectal pouch (P5).

779



780 (A)
781 **Fig. 6.** Internal armature of digestive tube in worker of *Apolemotermes fodiens* **sp. n.** Organs splayed on
782 slide. (A) Gizzard, showing five weakly developed pulvillar prominences (*arrows*). Direction of flow
783 downwards. (B) Enteric valve, showing six subequal, reticulated cushions bearing a very slight thickening
784 basally. Direction of flow upwards.
785



786
 787 **Fig. 7.** Internal armature of digestive tube in worker of two *Adaiphrotermes* species. (A) Gizzard,
 788 CIVT232. Note five swollen pulvilli bearing pectinated scales. Direction of flow downwards. (B) Enteric
 789 valve, CIVT232. The armature consists of six scaly pads originating in the funnel-like end of P1 and
 790 proceeding through a curved, narrow tubular section to the paunch entrance. Direction of flow upwards.
 791 (C) Enteric valve, BDIT4-3f1. Scaly pads bear tiny spines and follow a much shorter tube to the paunch
 792 than in the preceding species. Direction of flow upwards.

- 793
- 794 **Supporting Information**
- 795 **Appendix S1.** Revised identifications.
- 796 **Table S1.** Apicotermitinae samples used in this study.
- 797 **Table S2.** Species included as outgroups in this study.
- 798 **Figure S1.** Bayesian phylogenetic chronogram of Apicotermitinae inferred from mitochondrial genomes,
 799 with third codon positions included.
- 800 **Figure S2.** Bayesian phylogenetic tree of Apicotermitinae inferred from mitochondrial genomes.
- 801 **Figure S3.** Maximum-likelihood phylogenetic tree of Apicotermitinae inferred from mitochondrial
 802 genomes.
- 803 **Figure S4.** Ancestral biogeographic reconstruction for the Bayesian phylogenetic time-calibrated tree
 804 with third codon positions excluded.

805 **Figure S5.** Ancestral biogeographic reconstruction for the Bayesian phylogenetic time-calibrated tree
806 with third codon positions included.

807 **Figure S6.** Ancestral biogeographic reconstruction for the Bayesian phylogenetic tree of Apicotermitinae.

808 **Figure S7.** Ancestral biogeographic reconstruction for the Maximum likelihood phylogenetic tree of
809 Apicotermitinae.

810 **Figure S8.** Ancestral state reconstruction of soldier presence for the Bayesian phylogenetic tree of
811 Apicotermitinae using the Maximum Likelihood all-rate-different model.

812 **Figure S9.** Ancestral state reconstruction of soldier presence for the Bayesian phylogenetic tree of
813 Apicotermitinae using the Maximum Likelihood equal-rate model.

814 **Figure S10.** Ancestral state reconstruction of soldier presence for the Bayesian phylogenetic tree of
815 Apicotermitinae using the Maximum Likelihood symmetrical model.

816